

References

- ATTFIELD, J. P., SLEIGHT, A. W. & CHEETHAM, A. K. (1986). *Nature (London)*, **322**, 620–622.
- BAUR, W. H. (1974). *Acta Cryst.* **B30**, 1195–1215.
- BAUR, W. H. & KHAN, A. A. (1970). *Acta Cryst.* **B26**, 1584–1596.
- BERG, J.-E. & WERNER, P.-E. (1977). *Z. Kristallogr.* **145**, 310–320.
- CHEETHAM, A. K., DAVID, W. I. F., EDDY, M. M., JAKEMAN, R. J. B., JOHNSON, N. W. & TORARDI, C. C. (1986). *Nature (London)*, **320**, 46–48.
- FERRARIS, G. & FRANCHINI-ANGELA, M. (1972). *Acta Cryst.* **B28**, 3572–3583.
- FRENZ, B. A. (1978). *The Enraf-Nonius CAD-4 SDP – A Real-Time System for Concurrent X-ray Data Collection and Crystal Structure Solution*. In *Computing in Crystallography*, edited by H. SCHENK, R. OLTJOF-HAZEKAMP, H. VAN KONINGSVELD & G. C. BASSI, pp. 64–71. Delft Univ. Press.
- JOHNSON, C. K. (1965). *ORTEP*. Report ORNL-3794. Oak Ridge National Laboratory, Tennessee, USA.
- LANGFORD, J. I., LOUËR, D., SONNEVELD, E. J. & VISSER, J. W. (1986). *Powder Diffr.* **1**, 211–221.
- LEHMANN, M. S., CHRISTENSEN, A. N., FJELLVÅG, H., FEIDENHANS'L, R. & NIELSEN, M. (1987). *J. Appl. Cryst.* **20**, 123–129.
- LOUËR, D., DENEUVE, F. & OUIILLON, N. (1987). *Powder Diffr.* **2**, 253–254.
- LOUËR, D. & LOUËR, M. (1972). *J. Appl. Cryst.* **5**, 271–275.
- LOUËR, D. & LOUËR, M. (1987). *J. Solid State Chem.* **68**, 292–299.
- LOUËR, D. & VARGAS, R. (1982). *J. Appl. Cryst.* **15**, 542–545.
- RIETVELD, H. M. (1969). *J. Appl. Cryst.* **2**, 65–71.
- RUDOLF, P. & CLEARFIELD, A. (1985). *Acta Cryst.* **B41**, 418–425.
- SMITH, G. S. & SNYDER, R. L. (1979). *J. Appl. Cryst.* **12**, 60–65.
- SONNEVELD, E. J. & VISSER, J. W. (1975). *J. Appl. Cryst.* **8**, 1–7.
- WERNER, P.-E. (1986). *Chem. Scr. A*, **26**, 57–64.
- WILES, D. B. & YOUNG, R. A. (1981). *J. Appl. Cryst.* **14**, 149–151.
- WOLFF, P. M. DE (1968). *J. Appl. Cryst.* **1**, 108–113.
- YOUNG, R. A. & WILES, D. B. (1981). *Adv. X-ray Anal.* **24**, 1–23.

Acta Cryst. (1988). **B44**, 467–474

Electron Diffraction Observations from Some So-Called ‘LnMS₃’ Layer Compounds Isostructural with ‘~LaCrS₃’ and from Cannizzarite, ~Pb₄₆Bi₅₄S₁₂₇

BY T. B. WILLIAMS* AND B. G. HYDE

Research School of Chemistry, Australian National University, GPO Box 4, Canberra, ACT 2601, Australia

(Received 29 March 1988; accepted 23 May 1988)

Abstract

Electron diffraction data are reported and discussed for a series of so-called ‘LnMS₃’ compounds (Ln = La, Ce, Pr and Nd, M = Cr; Ln = La, M = Ti, V and Cr) and for cannizzarite (~46PbS.27Bi₂S₃). The structures of all these compounds consist of two layer types alternating along the stacking direction – which is the zone axis in most instances. In the first group the mismatch between the layers varies slightly (by up to 2.5%) as the cations are varied. In the last we find only the ~12/7 and 17/10 layer matches, and not their combinations 46/27 and 41/24 as reported by Matzat [*Acta Cryst.* (1979), **B35**, 133–136].

Introduction

There is a group of synthetic and mineral sulfosalts with apparently complex structures and large unit cells which can be simply described as consisting of stacks of two alternating layer types, *A* and *B*. One is a thin tetragonal [= (100)] section of NaCl type, the other a thin trigonal [= (111)] section of NaCl type. The complexity arises mainly from the incommensurability between their unit-layer vectors, but also from the

consequent small distortions (modulation) of the layers. Many examples of such cases of two interpenetrating substructures have been reviewed and described in some detail (Makovicky & Hyde, 1981) ranging from the most complex, such as cylindrite (~FePb₃Sn₄-Sb₂S₁₄) and the related franckeites (~FePb_{6-x}Sn_{2+x}-Sb₂S₁₄) and lengenbachite [~Pb₆(Ag,Cu)₂As₄S₁₃] to the simplest such as ‘~LaCrS₃’ and other ‘~LnMS₃’ (Ln = a rare-earth or yttrium cation). Their structural details are best explored by electron microscopy/diffraction (Williams & Hyde, 1988; Williams & Pring, in preparation). A previous paper (Otero-Diaz, Fitz Gerald, Williams & Hyde, 1985) included such an examination of ‘~LaCrS₃’; the purpose of the present paper is a similar examination, first of other ‘~LnMS₃’ and then of cannizzarite (~Pb₄₆Bi₅₄S₁₂₇).

‘~LnMS₃’

This group of structurally similar compounds is a particularly simple example of non-commensurate layer structures in which the pseudotetragonal layer *T* is two atom layers thick and the pseudo(ortho)hexagonal layer *O* is three atoms thick. Fig. 1 shows the monoclinic structure of ‘~LaCrS₃’ as reported by Kato, Kawada & Takahashi (1977) which has $a = 5.936$, $b = 5.752$, $c = 11.036$ Å, $\alpha = 90.39$, $\beta = 95.30$ and $\gamma = 90.02^\circ$

* Now at The Research Institute for Materials, Tohoku University, Sendai 980, Japan.

for T , $a = 5.936$, $b = 3.435$, $c = 11.053$ Å, $\alpha = 93.29$, $\beta = 95.29$ and $\gamma = 90.03^\circ$ for O and, for the true unit cell, $a = 5.94$, $b = 17.2$, $c = 66.2$ Å and $\alpha = 90.3$, $\beta = 95.3$, $\gamma = 90.0^\circ$. The style '~LaCrS₃' reflects the fact that there has been some argument about the exact stoichiometry of this compound: the non-commensurability between the two layer types suggested an ideal composition La₆Cr₅S₁₆ since, for the subcells, $a_T = a_O$, $c_T^* = c_O^*$, but $b_T \approx b_O \times 5/3$ and, for full occupancy of sites, the subcell contents are $T = 2\text{LaS}$, $O = \text{CrS}_2$. We believe that any doubt has now been resolved in favour of the more complicated formula (Otero-Diaz *et al.*, 1985), so that there is no need to invoke disorder on the La sites of the structure as was previously done (Kato *et al.*, 1977) in order to accommodate the simpler (but incorrect) stoichiometry 'LaCrS₃'.

Many other virtually isostructural '~LnMS₃' with Ln = La, Ce, Pr, Nd, Gd, Dy(?), Ho, Er as well as Y,

and/or $M = \text{Ti, V, Cr}$ have also been reported (Takahashi, Oka, Yamada & Ametami, 1971; Takahashi, Osaka & Yamada, 1973; Donohue, 1975; Murugesan, Ramesh, Gopalakrishnan & Rao, 1981; Serebrennikov & Alekseeva, 1981), but their structures have not been determined. We here describe the results of electron diffraction studies of some of these.

Experimental

High-purity lanthanide oxides in a graphite crucible were sulfided by r.f. induction heating in H₂S + Ar gas mixtures, first for 3 h at 1773 K and then for two periods totalling 6 h at 1473 K, with intermediate grinding and remixing. The products were always β -type (tetragonal) Ln₁₀S_{15-x}O_x, $0 \leq x \leq 1.0$ (Besançon, 1973; Besançon, Carré & Laruelle, 1973), which, at low temperatures, are apparently stabilized with respect to the stable orthorhombic α -type and pure sesquisulfide by oxygen contamination. (Our cell parameters for β -'La₂S₃' suggested $x \approx 0.92$ to 0.95.)

Transition-metal sulfides were prepared by synthesis from the elements, heated in evacuated and sealed silica ampoules at 1173 K for several days.

Appropriate sulfide mixtures (Ln/M $\approx 2/1$) were heated in silica tubes in similarly evacuated and sealed silica ampoules for 30 days at 1273 K. After grinding the products they were returned to similar containers with iodine (5 mg cm⁻³), and chemical transport attempted for several weeks. Only the La-Cr compound was transported successfully. In the other cases a mass of smaller, often lamellar crystallites was produced by mineralization. All had a similar appearance, dark grey and metallic. (In transmitted light the lamellar ~LaCrS₃ was ruby red, and occasionally the crystals were curved rather than flat.) Platelike crystals were selected for study.

All X-ray powder diffraction patterns (from a Guinier-Hägg camera with Cu K α_1 radiation) were similar, suggesting similar structures in all cases. (Because of strongly preferred orientation – a consequence of the highly lamellar nature of the crystals – intensity measurement is futile and was not attempted.)

Electron microscopy samples were prepared by dispersing the lamellar crystals in ethanol using a 400 W ultrasonic probe, followed by deposition on a 'holey carbon' support grid. These were examined in Jeol 100 CX and 200 CX microscopes.

Because the crystalline products of the syntheses were so thin (tens of μm) attempts to prepare (100) and (010) sections were unsuccessful. Hence, because of their extreme lamellar morphology, almost all low-index-zone-axis diffraction patterns were [001] [in contrast to cylindrite *etc.* in Williams & Hyde (1988)]. Images in this zone are singularly uninformative, and so we are largely restricted to a consideration of their diffraction patterns.

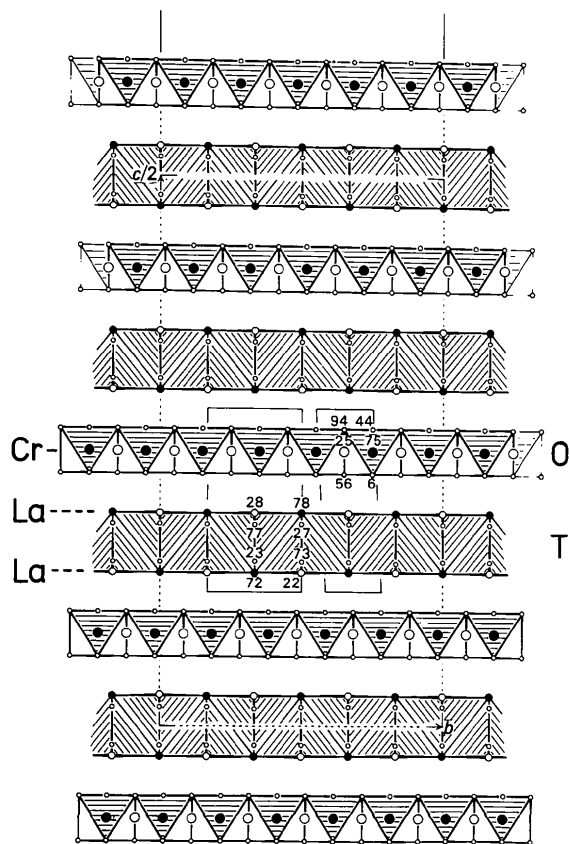


Fig. 1. The structure of 'LaCrS₃' according to Kato *et al.* (1977) projected along a . Four pseudo-tetragonal T layers and five pseudo-orthohexagonal O layers are drawn; the outline of half the unit cell, *i.e.* three layer-pairs in the c direction and the full $3b_T : 5b_O$ match is indicated by broken lines. The subcell outlines are indicated by full lines, and illustrate the different stackings of the T and O layers. Small circles are S-atom positions, medium circles are La, and large circles are Cr: the atom heights are given as a percentage of a . Cr-centred octahedra (O layer) and S-centred square pyramids (T layer) are shaded.

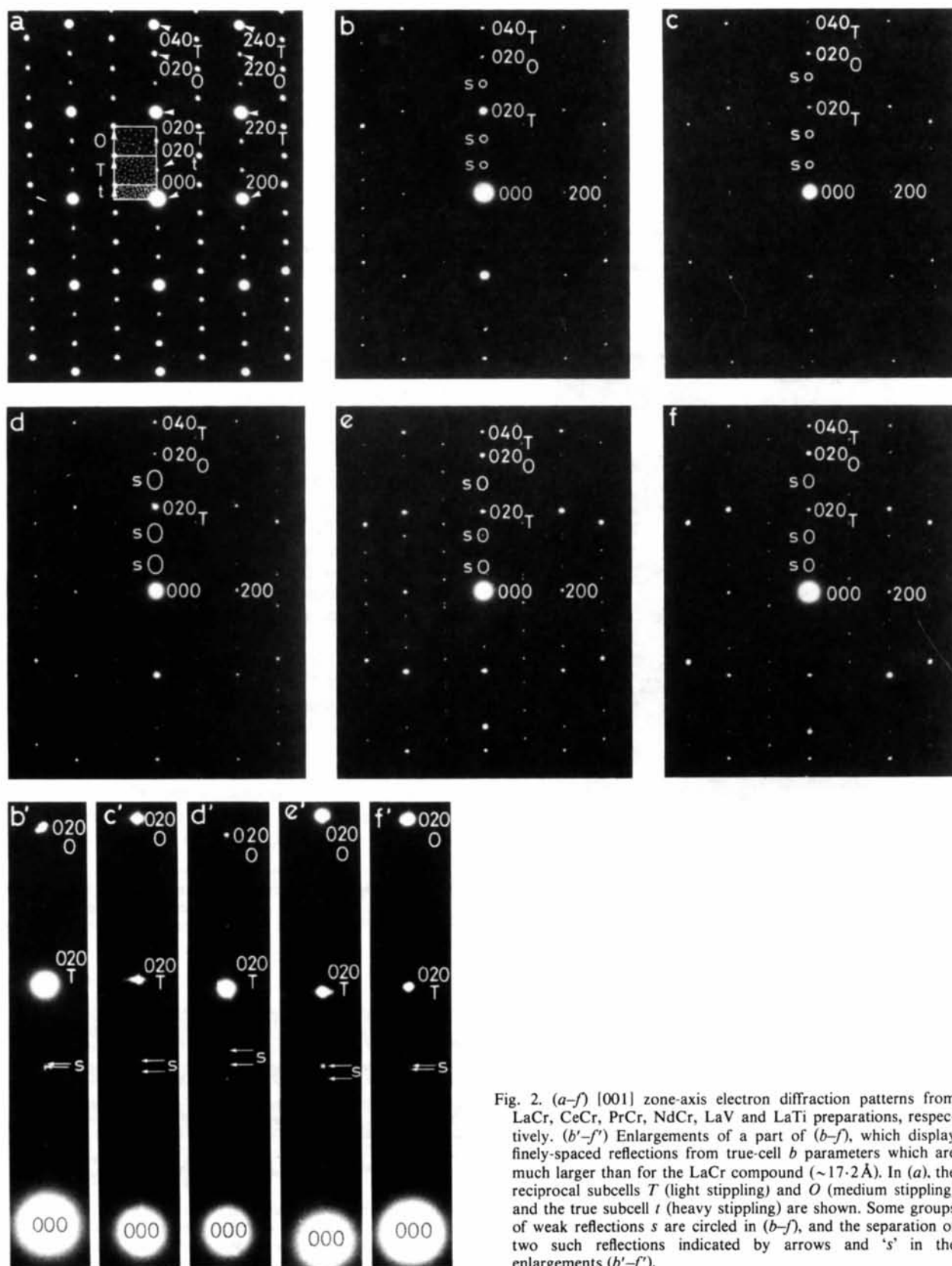


Fig. 2. (a-f) [001] zone-axis electron diffraction patterns from LaCr, CeCr, PrCr, NdCr, LaV and LaTi preparations, respectively. (b'-f') Enlargements of a part of (b-f), which display finely-spaced reflections from true-cell b parameters which are much larger than for the LaCr compound ($\sim 17.2 \text{ \AA}$). In (a), the reciprocal subcells T (light stippling) and O (medium stippling) and the true subcell t (heavy stippling) are shown. Some groups of weak reflections s are circled in (b-f), and the separation of two such reflections indicated by arrows and 's' in the enlargements (b'-f').

Table 1. Mismatch between b_T and b_O from measurement of [001] diffraction patterns of '~LnMS₃'

LnM=	LaCr	CeCr	PrCr	NdCr	LaV	LaTi
Ratio b_T/b_O (from all reflections along b^*)	5/3 =1.66 ₇	123/74† =1.66 ₂	41/25 =1.64 ₀	26/16 =1.62 ₅	34/20 =1.70 ₀	99/59† =1.67 ₈
$R(020)_O/R(020)_T=b_T/b_O$	1.66 ₈	1.66 ₀	1.63 ₄	1.62 ₇	1.70 ₂	1.67 ₆
b_i (Å)‡ (= numerator × b_T = denominator × b_O = n and d from line 1)	~17 ₂	~42 ₃	~14 ₃	~89 ₇	~115 ₀	~33 ₉
Formula of '~LnMS ₃ ' corresponding to line 2	La ₁₋₂₀ CrS ₃₋₂₀	Ce ₁₋₂₀ CrS ₃₋₂₀	Pr ₁₋₂₀ CrS ₃₋₂₀	Nd ₁₋₂₃ CrS ₃₋₂₃	La ₁₋₁₇ VS ₃₋₁₇	La ₁₋₁₉ TiS ₃₋₁₉
Average cation valence	2.90 ₄	2.90 ₄	2.90 ₁	2.89 ₆	2.91 ₀	2.91 ₂

† These values, in particular, are obviously prone to error because the multiplicities are so high.

‡ Accurate values for these cannot be obtained from electron diffraction patterns because of unavoidable variations (of several percent) in the camera constant of the electron microscope. They have been calculated from the ratios b_T/b_O (in line 1) assuming $b_T = 5.75_2$ Å for LaMS₃ or $b_O = 3.43_3$ Å for LnCrS₃ [both as determined for LaCrS₃ by Kato *et al.* (1977)].

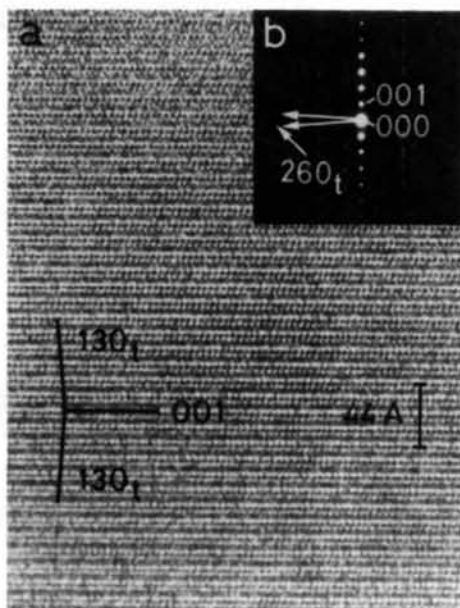


Fig. 3. (a) Image and (b) corresponding [310] zone-axis diffraction pattern from an area of LaCr preparation. The rows of horizontal contrast in (a) correspond to sections of T layers (black dots) and O layers (unresolved). Traces of $(130)_t \equiv (110)_T$ and of (001) planes are shown. The crystal is twinned, as the diffraction pattern confirms. The streaking in (b) arises from the (001) composition planes [one only appears in (a)].

Results and discussion

A typical [001] zone-axis pattern from each preparation is shown in Fig. 2. The simplest is that for '~LaCrS₃' (Fig. 2a) which is identical to that previously published (Otero-Diaz *et al.*, 1985). It confirms the C -centring of the T and O subcells and of the true unit cell, t . As far as one can tell the true cell reflections are unsplit, so that $b_T/b_O = 5/3$ exactly; a relation which would appear to be confirmed by the relatively high intensity of these reflections.

In all the other patterns, groups of two or three closely spaced, weak reflections (rather than single, stronger reflections) appear close to the positions $n/3 \times (020)_T$ ($n \bmod 3 \neq 0$) = $m/5 \times (020)_O$ ($m \bmod 5 \neq 0$); cf. Figs. 2(b-f) and, especially, 2(b'-f'), where some are marked 's'. This indicates that in these cases b_T/b_O is close to but not exactly 5/3; the difference is very little in the case of '~CeCrS₃' and '~LaTiS₃' but more in the other cases. Careful measurements of the positions of the reflections (for T , O and t) along b^* , and assuming that b_T^* is an integral submultiple of b_T^* and b_O^* † leads to the ratios b_T/b_O and

† This assumption is not important. There is always an irrational number (corresponding to a truly incommensurate structure) insignificantly different from a ratio of integers; but the reverse is equally true.

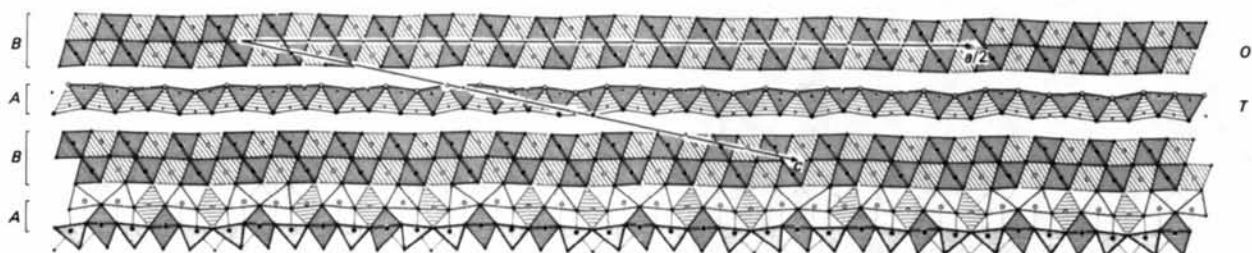


Fig. 4. [010] projection of the cannizzarite structure (Matzat, 1979). Slightly more than half of one unit cell is drawn; the full ~74 Å c repeat and half the ~190 Å true-cell a . Two layers of each kind (A and B) are drawn, with cation-centred octahedra (both B layers), and both S -centred (upper A layer) and cation-centred (lower A layer) polyhedra drawn to emphasize the intralayer (upper A) and interlayer (lower A) bonding. Puckering or undulation of the layers is evident. Atom heights are $0.25b$ (open circles) and $0.75b$ (filled circles).

the values b_i given in Table 1, which are estimated to be accurate to better than $\sim 0.5\%$. The first two rows of numbers in the table are from all reflections; the third row is from only the subcell reflections 020_o and 020_r ; the fourth row is a calculated, approximate b_i (subcell b_o and b_r values are not very accurately known). Clearly, the agreement between the two values of the ratio b_r/b_o is satisfactory. The measured ratios in the second row of Table 1 differ from $5/3$ by approximately 0, -0.3 , -1.6 , -2.5 , 2.0 and 0.7% respectively. Except for LaCr however, the values of b_i are *much* less certain. (A small change in the ratio b_r/b_o can give a very large change in b_r .) But all b_i values are large (except for LaCr).

LnCrS_3 , Ln = La, Ce, Pr, Nd. Other things (e.g. valences) being equal, the bond length Ln-S decreases along this series. In the crudest terms therefore, one might expect b_r to decrease, and hence b_r/b_o also. This is in accord with the observations.

LaMS_3 , $M = \text{Ti, V, Cr}$. By analogy with the previous paragraph one might expect the ratio b_r/b_o to increase in the sequence $\text{Ti} \rightarrow \text{V} \rightarrow \text{Cr}$ (as the bond length $M-S$ decreases). But this is not so; the respective values being 1.67_8 , 1.70_0 , 1.66_7 . The anomaly is significantly greater than the experimental error.

But the crudest terms are not good enough. For a_o to equal a_r there must be some adjustment of $S-M/\text{Ln}-S$ bond angles and/or lengths as Ln and/or M are varied. It is possible that the greatest flexibility is in the O layer – where the height of each MS_6 octahedron can change (within reason) as its area [in the (001) plane] changes, while retaining constant bond lengths. (This is clearly seen in the c/a ratios of many CdCl_2 - and $\text{Cd}(\text{OH})_2$ -type structures.) But we do not have sufficient data of sufficient accuracy to explore this.

Since in any given ' $\sim \text{LnMS}_3$ ' the subcell parameters a and c^* [or $d(001)$] are clearly identical for both subcells T and O , it follows (if substitutional disorder between Ln and M is neglected, as we believe it should be) that the stoichiometry is determined by the ratio, $r = b_r/b_o$. It should be $2\text{LnS}.r\text{MS}_2$ (as is clear from Fig. 1), or $(2/r)\text{LnS}.MS_2 = \text{Ln}_{2/r}\text{MS}_{2+(2/r)}$. These latter values are given in line 5 of Table 1. None is LnMS_3 . Hence, all average cation valences (calculated by assuming only S^{2-}) are somewhat less than 3.00 – which is not unexpected given the preparation conditions of the sulfides: the binaries also have cation valences less than 3 ($\sim 2.7+$ for Ln, $2.4+$ for Cr).

In conclusion it should be emphasised that bond length is not the only geometrical factor involved in these compounds and their structures, and that geometry is by no means the only variable parameter. Since the mismatch determines the stoichiometry $\text{Ln}_{1+x}\text{MS}_{3+x}$ and the stoichiometry determines the average cation valence $[= 2(3+x)/(2+x)]$ then in hindsight it seems likely that a variation in sulfur activity during the preparation (and it was not controlled) will affect the

average cation valence and, given that the structure consists of LnS and MS_2 layers, the stoichiometric ratio $\text{Ln}/M = 1+x$ also. This thermodynamic aspect of the behaviour of these systems has yet to be explored.

Our only useful result with a zone axis other than [001] is for the LaCr preparation. Shown in Fig. 3, its zone axis is $[3\bar{1}0]_t = [1\bar{1}0]_r$. The diffraction spots (Fig. 3b) are streaked, and reveal twinning [by reflection in (001), as previously reported by Kato *et al.* (1977)], with a preponderance of one twin. The corresponding image (Fig. 3a) confirms this, as seen by the orientations of the traces of $(130)_r$. This image clearly exhibits (001) layer stacking, the contrast showing two alternating types of rows – the projected T and O layers. The repeat distance along $[3\bar{1}0]_t$ is rather long for reliable image simulation ($\sim 24.4 \text{ \AA}$); but the image may be plausibly interpreted in a naive way because $(130)_t = (110)_r$. The interplanar spacing $d(130)_t = d(110)_r = 4.12 \text{ \AA}$, which corresponds to the spacing of the black dots resolved in the horizontal rows of the image – the measured value of which [using $d(001) = 11.0 \text{ \AA}$ as internal standard] is 4.0_4 \AA . These rows therefore correspond to the T layers. The intervening lines of dark contrast are not resolved, which is to be



Fig. 5. Scanning electron microscope image of synthetic 'cannizzarite'. The larger, bladelike crystals are cannizzarite, whilst the finer material is a mixture of cannizzarite and bismuthinite, Bi_2S_3 . The extreme thinness and fragility of the crystals is evident in this image; most crystals are bent and the cannizzarite is both frayed and transparent to the 20 kV electrons used in this study.

expected since they should correspond to the *O* layers with $(530)_O \parallel (130)_T$ and $d(530)_O = 0.82 \text{ \AA}$ – well below the resolving power of the microscope.

Cannizzarite, $\sim \text{Pb}_{46}\text{Bi}_{54}\text{S}_{127} = \sim 46\text{PbS} \cdot 27\text{Bi}_2\text{S}_3$

The first description of this mineral species (Zambonini, de Fiore & Carobbi, 1925) preceded its structure determination (Matzat, 1979) by more than 50 years, and its synthesis (Graham, Thompson & Berry, 1953) by about 25 years. These intervals reflect its structural complexity although once again it is simple in principle. Two interpenetrating substructures arise from the interleaving of two types of layers: a two-atom-thick pseudotetragonal layer, *T* [(100)_{NACl}-type] and a five-atom-thick pseudo-hexagonal layer, *O* [(111)_{NACl}-type]. As in ' $\sim \text{LnMS}_3$ ', the former consists of edge-shared square pyramids, but the latter is two octahedra thick (instead of one), cf. Fig. 4 (after Matzat, 1979). The true unit cell is rather large and oddly shaped: monoclinic, $P2_1/m$, with $a = 189.8$, $b = 4.09$, $c = 74.06 \text{ \AA}$, $\beta = 11.93^\circ$, contents = $2 \times (\sim \text{Pb}_{46}\text{Bi}_{54}\text{S}_{127})$. The subcells are: $a = 4.13$, $b = 4.09$, $c = 15.48 \text{ \AA}$, $\beta = 98.56^\circ$ for *T*, and $a = 7.03$, $b = 4.09$, $c = 15.46 \text{ \AA}$, $\beta = 98.00^\circ$ for *O*; both also $P2_1/m$. The *T*-layer stoichiometry is $(\text{Pb}_{30}\text{Bi}_{16}\text{S}_{46})^{16+}$ and that of the *O* layer is $(\text{Pb}_{16}\text{Bi}_{38}\text{S}_{81})^{16-}$. The large *a* parameter of the true cell corresponds to the match $46 \times a_T = 27 \times a_O$; and $b_T = b_O$.†

Although very similar in structure to ' $\sim \text{LnMS}_3$ ', the differences are interesting: (i) and most obviously, the difference in the *O*-layer thickness; (ii) the orientation of the *T* layers (relative to that of *O*) differs by 45° ; (iii) the misfit directions for the *O* layers differ by 90° (compare Fig. 4 with Fig. 1 for ' $\sim \text{LaCrS}_3$ '). Also, (iv) the stacking unit is in this case just one pair of layers [instead of the six pairs reported for ' $\sim \text{LaCrS}_3$ ' (Kato *et al.*, 1977)]. Notice also the undulations (in the \mathbf{c}^* direction) of the layers in cannizzarite (Fig. 4): this is more plausible than the planar layers reported for ' $\sim \text{LaCrS}_3$ ' (Fig. 1; Kato *et al.*, 1977).

For cannizzarite, Graham *et al.* (1953) reported $12 \times a_T = 7 \times a_O$. Matzat (1979) suggested that this was only a subcell of the true unit cell, and that there was also a second large subcell with $17 \times a_T =$

$10 \times a_O$.† His large true cell is then $(12 \times a_T) + 2(17 \times a_T) = (7 \times a_O) + 2(10 \times a_O)$ or $46 \times a_T = 27 \times a_O$. He also reported a related, synthetic 'cannizzarite' in which $2(12 \times a_T) + (17 \times a_T) = 2(7 \times a_O) + (10 \times a_O)$ or $41 \times a_T = 24 \times a_O$. The multiplicity ratios are then $46/27 = 1.703_7$ for the first and $41/24 = 1.708_3$ for the second: a small difference. For the two subcells they are $12/7 = 1.714$ and $17/10 = 1.700$. Divided by the last the resulting ratios are 1.002_2 , 1.004_9 , 1.008_4 and 1.000 – a total range of $< 1\%$. Clearly, variation in the a_T/a_O match is feasible, and likely to be related to the stoichiometric ratio Pb:Bi (Makovicky & Hyde, 1981). Electron diffraction patterns with a \mathbf{c}^* zone axis are therefore of some interest.

Experimental

Only one natural specimen of cannizzarite was available to us – small, extremely thin, lath-shaped crystals on the surface of a vuggy, volcanic silicate specimen from the type locality, Vulcano (Italy); a $2 \times 2 \times 2 \text{ cm}$ chip from sample R4089, kindly provided by the Smithsonian Institute (Washington, DC). Accordingly, synthesis was attempted, using the hydrothermal method of Graham *et al.* (1953). Only one preparation was successful: it contained small clusters of laths and a large amount of fibrous material (Fig. 5). Scanning electron microscopy revealed that the former resembled cannizzarite, and that the latter was Bi_2S_3 . This was confirmed by X-ray powder diffraction.

The lath-like crystals (synthetic and natural) were studied by electron diffraction, as described above for ' $\sim \text{LnMS}_3$ '.

Results and discussion

Only approximate \mathbf{c}^* zone-axis patterns could be obtained and, again, exact orientation was not possible because the crystals were so thin and, to a degree, the patterns therefore independent of tilt angle. Some typical results are shown in Figs. 6(*a-c*) and 6(*a'-c'*), the first two samples being synthetic and the last natural. At first sight, the distribution of the intensity over the various reflections appears odd; probably because of inexact orientation. In *a*, for example, the stronger reflections 200_T , 200_O , 020 and $\pm 110_T$ and $\bar{1}10_T$ are clear: some additional, fairly strong reflections appear, e.g. those close to ± 010 . Thus the subcell reflections are again identifiable and hence the ratios of the resulting subcell parameters can be determined. All the latter are rather similar:

- (a) $a_O/b = 1.71$, $a_T/b = 1.00_2$, $a_O/a_T = 1.70_5$;
- (b) $a_O/b = 1.72_8$, $a_T/b = 1.00_9$, $a_O/a_T = 1.71_3$;
- (c) $a_O/b = 1.74_6$, $a_T/b = 1.01_5$, $a_O/a_T = 1.72$;

† These subcells are not to be confused with the *O* and *T* subcells referred to earlier.

† Graham *et al.* (1953) also reported the presence of an additional phase (phase 3) in the product of their synthesis. It resembled cannizzarite (phase 2) in habit, diffraction pattern and cell dimensions, except that its layer-pair thickness was greater by $\sim 3.3 \text{ \AA}$: $c_T \sin \beta = 18.54 \text{ \AA}$ compared with 15.31 (natural) and 15.20 \AA (synthetic) for cannizzarites. This corresponds to an extra *MX* layer, but whether to *T* or *O* is difficult to determine in the absence of further information such as an analysis. From the Matzat structure in Fig. 3 one can measure thickness changes of $\sim 3.5 \text{ \AA}$ for an additional plane of atoms in a *T* layer, and $\sim 3.3 \text{ \AA}$ for an additional octahedral layer to *O*: hardly unequivocal but perhaps slightly in favour of a three-octahedron-thick *O* layer, as proposed by Matzat (1979).

the first two columns being reasonably close to the ideal values for orthohexagonal and tetragonal subcells, $\sqrt{3}$ and 1.

In addition, there are many weaker ('superlattice') reflections aligned along \mathbf{a}^* , see especially Figs. 6(a' - c'). Careful measurement of these shows that

within the error of measurement ($\sim 1\%$) the smallest interval between them is (a') $a_T^*/17 = a_O^*/10$, (b') $a_T^*/12 = a_O^*/7$, and (c') $a_T^*/12 = a_O^*/7$ also. These ratios correspond to the two substructures recognised by Matzat (1979) and referred to above and, within experimental error, agree with those listed for a_O/a_T .

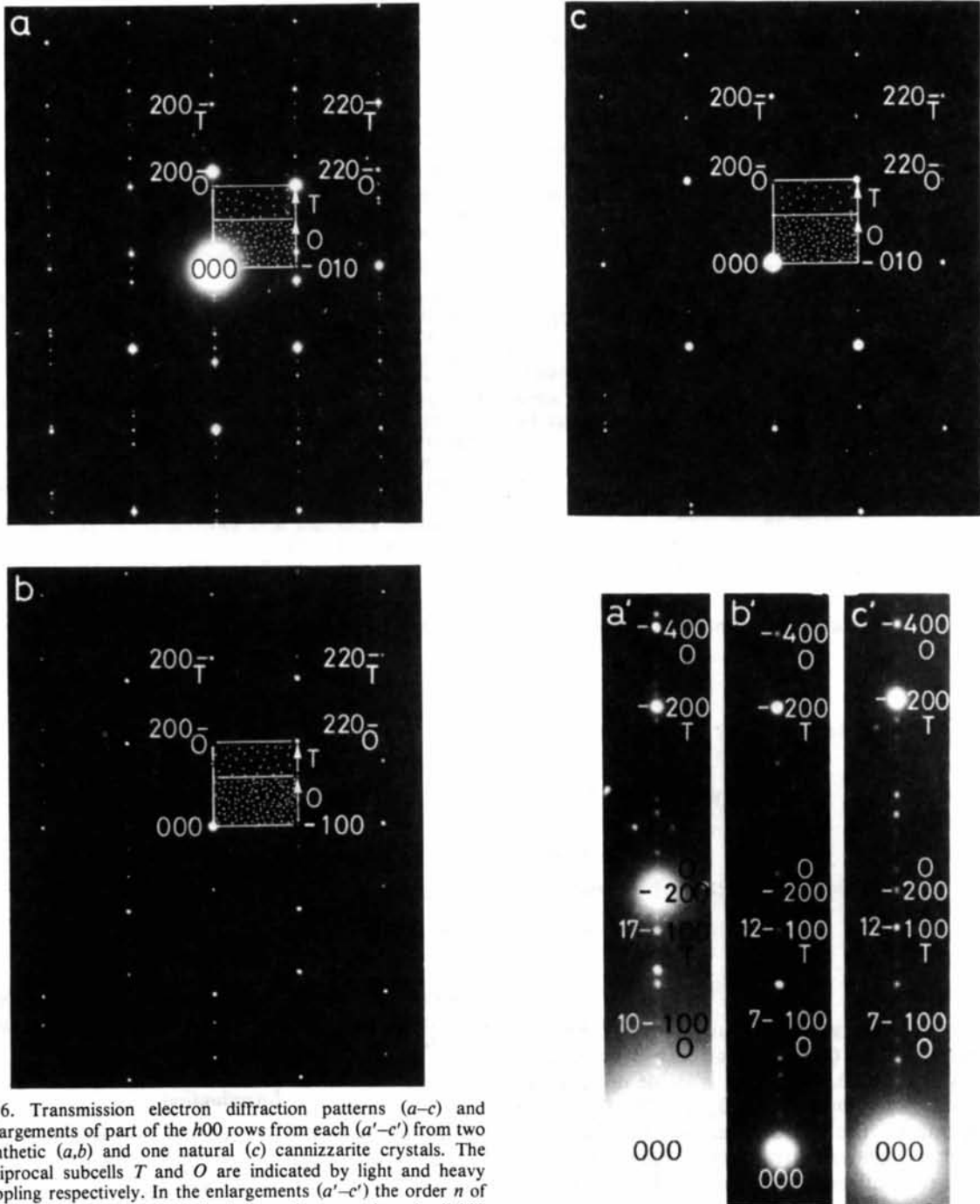


Fig. 6. Transmission electron diffraction patterns (a - c) and enlargements of part of the $h00$ rows from each (a' - c') from two synthetic (a, b) and one natural (c) cannizzarite crystals. The reciprocal subcells T and O are indicated by light and heavy stippling respectively. In the enlargements (a' - c') the order n of the true-cell reflections $h_n 00$ is shown adjacent to the subcell 100 reflections.

Fig. 6 (cont.)

Whether the 'superlattice' spots correspond to the *a* axis of the true unit cell [as the 12:7 case was reported to be by Graham *et al.* (1953)] or only to one of the large subcells proposed by Matzat cannot be determined definitively from these measurements which, at $\pm 1\%$, are insufficiently precise. The enlargements, Figs. 6($a'-c'$), do not help in this respect. That the intervals 17/10 and 12/7 dominate the diffraction patterns (irrespective of the exact measurements), and that there are no additional (more closely spaced) reflections, strongly suggests that each true structure is (at least) dominated by one of these substructures. Since our selected-area diffraction patterns come from very small volumes of crystal (compared with that required for X-ray diffraction) it may well be that the two substructures are true (local) structures; and that a large crystal (as used for X-ray diffraction) may be a heterogeneous mixture of the two. Certainly there is no evidence here for the larger cell, $46 \times a_T = 27 \times a_O$, reported by Matzat.

This implies that the stoichiometries are 17PbS.₁₀Bi₂S₃ for (*a, a'*) and 12PbS.₇Bi₂S₃ for (*b, b'*) and (*c, c'*), *i.e.* $\sim \text{PbBi}_{1.176}\text{S}_{2.765}$ and $\sim \text{PbBi}_{1.167}\text{S}_{2.750}$ instead of Matzat's $\sim \text{PbBi}_{1.174}\text{S}_{2.761}$. Again these are very small variations: only $\sim 0.2\%$ and $\sim 0.6\%$ for Bi, and $\sim 0.1\%$ and $\sim 0.4\%$ for S (relative to Pb).

Concluding remarks

In the 'LnMS₃' cases we again find no evidence of disorder [*cf.* Otero-Diaz *et al.* (1985)], apart from twinning on (001). The variation in the b_T/b_O mismatch with change in Ln and/or *M* seems to us to support the

earlier suggestion (Otero-Diaz *et al.*, 1985) that there is no other disorder (*e.g.* empty Ln sites or *M* on Ln sites). It follows that none of these has stoichiometry LnMS₃, but rather $\sim \text{Ln}_{1.2}\text{MS}_{3.2}$.

In synthetic and natural cannizzarite we find the two basic, layer mismatches $a_O/a_T = 12/7$ and $17/10$, but no evidence for their combinations $46/27 = (12 + 2 \times 17)/(7 + 2 \times 10)$ or $41/24 = (2 \times 12 + 17)/(2 \times 7 + 10)$, as proposed by Matzat (1979).

References

- BESANÇON, P. (1973). *J. Solid State Chem.* **7**, 232–240.
 BESANÇON, P., CARRÉ, D. & LARUELLE, P. (1973). *Acta Cryst.* **B29**, 1064–1066.
 DONOHUE, P. C. (1975). *J. Solid State Chem.* **12**, 80–83.
 GRAHAM, A. R., THOMPSON, R. M. & BERRY, L. G. (1953). *Am. Mineral.* **38**, 536–544.
 KATO, K., KAWADA, I. & TAKAHASHI, T. (1977). *Acta Cryst.* **B33**, 3437–3443.
 MAKOVICKY, E. & HYDE, B. G. (1981). *Struct. Bonding (Berlin)*, **46**, 101–170.
 MATZAT, E. (1979). *Acta Cryst.* **B35**, 133–136.
 MURUGESAN, T., RAMESH, S., GOPALAKRISHNAN, J. & RAO, C. N. R. (1981). *J. Solid State Chem.* **38**, 165–172.
 OTERO-DIAZ, L., FITZ GERALD, J. D., WILLIAMS, T. B. & HYDE, B. G. (1985). *Acta Cryst.* **B41**, 405–410.
 SEREBRENNIKOV, V. V. & ALEKSEVA, T. P. (1981). *Russ. J. Inorg. Chem.* **26**, 837–838.
 TAKAHASHI, T., OKA, T., YAMADA, O. & AMETAMI, K. (1971). *Mater. Res. Bull.* **6**, 173–182.
 TAKAHASHI, T., OSAKA, S. & YAMADA, O. (1973). *J. Phys. Chem. Solids*, **34**, 1131–1135.
 WILLIAMS, T. B. & HYDE, B. G. (1988). *Phys. Chem. Miner.* In the press.
 ZAMBONINI, F., DE FIORE, O. & CAROBBI, G. (1925). *Rend. Accad. Sci. Fis. Nat. Naples Ser. 3*, **31**, 24–29.

Acta Cryst. (1988). **B44**, 474–480

A New Pseudo-Binary Tungsten Oxide, W₁₇O₄₇

BY M. M. DOBSON AND R. J. D. TILLEY

Department of Materials, University College, Newport Road, Cardiff CF2 1TA, Wales

(Received 22 January 1986; accepted 8 April 1988)

Abstract

A new pseudo-binary tungsten oxide which has the composition W₁₇O₄₇ (WO_{2.765}) has been discovered in the Sb–W–O system. The phase is stable up to about 1233 K and decomposes to W₁₈O₄₉ and W₂₄O₂₈ above this temperature. The approximate structure has been determined by high-resolution electron microscopy and powder X-ray diffraction methods. The monoclinic unit-cell parameters are $a = 18.84$, $b = 3.787$, $c = 12.33$ Å, $\beta = 102.67^\circ$, $Z = 1$, space group $P2/m$. The

structure is built up of octahedra and pentagonal columns linked in such a way as to form hexagonal tunnels.

Introduction

Tungsten trioxide has a crystal structure which can be described as being built up from slightly distorted octahedra arranged so as to share corners. Reduction of WO₃ to compositions below approximately WO_{2.87} results in the formation of structures which are built up from WO₇

0108-7681/88/050474-07\$03.00

© 1988 International Union of Crystallography